Citation: Cell Death and Disease (2013) 4, e506; doi:10.1038/cddis.2013.28

www.nature.com/cddis

Inhibition of H3K9 methyltransferases G9a/GLP prevents ototoxicity and ongoing hair cell death

H Yu[1,5], Q Lin[1,5], Y Wang[1], Y He[2], S Fu[3], H Jiang[3], Y Yu[3], S Sun[4], Y Chen[4], J Shou*[,3] and H Li*[,1,2]

Sensorineural hearing loss (SNHL) is one of the most common sensory defects in humans. Hair cells are vulnerable to various ototoxic insults. Effective prevention of hair cell loss remains an unmet medical need. Apoptotic hair cell death, which involves active regulation of transcription, accounts for the majority of aminoglycoside-induced hair cells loss. As one of the important epigenetic covalent modifications, histone methylation is involved in the regulation of gene expression, development and reaction to injury. In particular, H3K9 dimethylation (H3K9me2) is critical for euchromatin gene silencing. In the present study, we examined the roles of two highly homologous histone methyltransfereases responsible for this modification, G9a/G9a-like protein (GLP), in the reaction to aminoglycoside-induced hair cell damage. We observed a rapid increase of H3K9me2 upon hair cell damage in organotypic cochlear cultures. Treatment with the G9a/GLP-specific inhibitors, BIX01294 or UNC0638, reduced the level of H3K9me2 and prevented hair cells from death. Local delivery of BIX01294 also prevented neomycin-induced *in vivo* auditory hair cell loss in the organ of Corti in a mouse damage model. It is unlikely that BIX01294 functions through blocking aminoglycoside absorption as it does not interfere with aminoglycoside uptaking by hair cells in the organotypic cochlear cultures. Our data revealed a novel role of histone methylation in otoprotection, which is of potential therapeutic value for SNHL management.

Cell Death and Disease (2013) **4,** e506; doi:10.1038/cddis.2013.28; published online 21 February 2013
Subject Category: Neuroscience

As one of the most common sensory defects in humans, sensorineural hearing loss (SNHL) occurs in $>50\%$ of individuals between 50 and 80 years of age and affects $>30{,}000$ children annually,[1] largely due to the vulnerability of the sensory hair cells. The leading cause of SNHL is permanent inner ear hair cell damage; as mammalian hair cells are incapable of spontaneous self-regeneration.[2] Potential remedies to SNHL thus include protection from hair cell apoptosis and induced hair cell regeneration.[3,4] However, effective regeneration of functional hair cells remains scientifically challenging. Therefore, active protection of cochlear hair cells is of critical importance for SNHL management.

Discordant disease susceptibilities have been shown in monozygotic twins despite their shared genetic background. The underlying molecular mechanism is believed to involve epigenetic modifications of the genome, characterised by dynamic changes in DNA methylation and noncoding RNAs, as well as diverse patterns of covalent histone modifications.[5] Recently, certain microRNAs were found to be associated with the onset and progression of deafness in the diminuendo mouse model, which showed progressive hearing loss starting from an early age,[6] indicating a role of epigenetic regulation in hearing biology.

Epigenetic modifications have an important role in the regulation of many chromosomal functions and are closely linked to certain biological events, such as transcriptional regulation, cell survival, differentiation, and cell death.[7–10] Dimethylation of lysine 9 of histone H3 (H3K9me2) is a dynamic histone methylation mark associated with euchromatin gene silencing. Change of H3K9me2 is implicated in both embryogenesis and carcinogenesis.[11–13] With the development of potent and selective G9a and G9a-like protein (GLP) inhibitors, such as BIX01294 and UNC0638,[14,15] it is possible to probe the G9a/GLP-mediated functions of H3K9me2 in detail through pharmacological inhibition.[14,16] Notably, inhibition of G9a by the administration of BIX01294 led to the suppression of cell migration and invasion in certain types of infinitely proliferous cancer cells.[17,18] However, the involvement of histone methylation in the fate determination of mammalian hair cells and the effects of H3K9me2 in terminally differentiated hair cells are still poorly understood.

[1]Department of Otolaryngology, Affiliated Eye and ENT Hospital, Fudan University, Shanghai, China; [2]Institutes of Biomedical Sciences, Fudan University, Shanghai, China; [3]China Novartis Institutes for BioMedical Research, Shanghai, China and [4]Department of Lab Centre, Affiliated Eye and ENT Hospital, Fudan University, Shanghai, China
*Corresponding author: J Shou, Novartis Institutes for BioMedical Research, Shanghai 201203, China. Tel: +86 18621082589; Fax: +86 21 61606155; E-mail: jianyong.shou@novartis.com
or H Li, Department of Otolaryngology, Affiliated Eye and ENT Hospital, Fudan University, Shanghai 200031, China. Tel: +86 21 64377134; Fax: +86 21 64377151; E-mail: huaweili2000@163.com
[5]These two authors contributed equally to this work.
Keywords: organ of Corti; ototoxicity; susceptibility; apoptosis; epigenetic regulation
Abbreviations: GLP, G9a-like protein; GTTR, gentamicin tagged with Texas Red; H3K9me2, dimethylation of lysine 9 of histone H3; SEM, scanning electron microscope; SNHL, sensorineural hearing loss; TMRM, tetramethylrhodamine methyl ester
Received 05.11.12; revised 06.1.13; accepted 07.1.13; Edited by H-U Simon

In the present study, we analysed the involvement of H3K9me2 in the susceptibility of hair cells to injury. Our data showed that H3K9me2 rapidly increased following hair cell damage induced by aminoglycosides and preceded the death of the hair cells. Inhibition of G9a/GLP protected the auditory hair cells from death in neonatal organ of Corti explants *in vitro*. Pre-conditioning with BIX01294 also prevented hair cell loss induced by neomycin *in vivo* and improved hearing threshold. Suppression of H3K9me2 induced by ototoxic drugs may provide an effective way of clinical importance to protect hair cells from injury.

Results

Aminoglycoside induced a rapid increase of H3K9me2 in hair cell-injury models. Histone methylation has important roles in transcription regulation, genome integrity, and epigenetic inheritance. We first examined the pattern of H3K9me2 in normal cochlear epithelium using immunohistochemistry. H3K9me2 staining showed a punctate distribution in virtually all the hair cells, with the strongest signal observed at the edge of outer hair cells and a downward gradient leading to dramatically decreased staining in the inner hair cells (Figure 1a).

We next examined H3K9me2 level in the cochlear epithelium upon damage in a neonatal neomycin-induced ototoxicity model. The global level of H3K9me2 was measured following neomycin incubation of different durations. We observed a significant increase of H3K9me2 staining in the organ of Corti without apparent hair cell loss after 15 min of incubation with 1 mM neomycin (Figure 1b). This elevated level of H3K9me2 remained in the organ of Corti up to 3 h after treatment (Figure 1c), but disappeared after 24 h of treatment, largely due to the loss of hair cells that followed (data not shown).

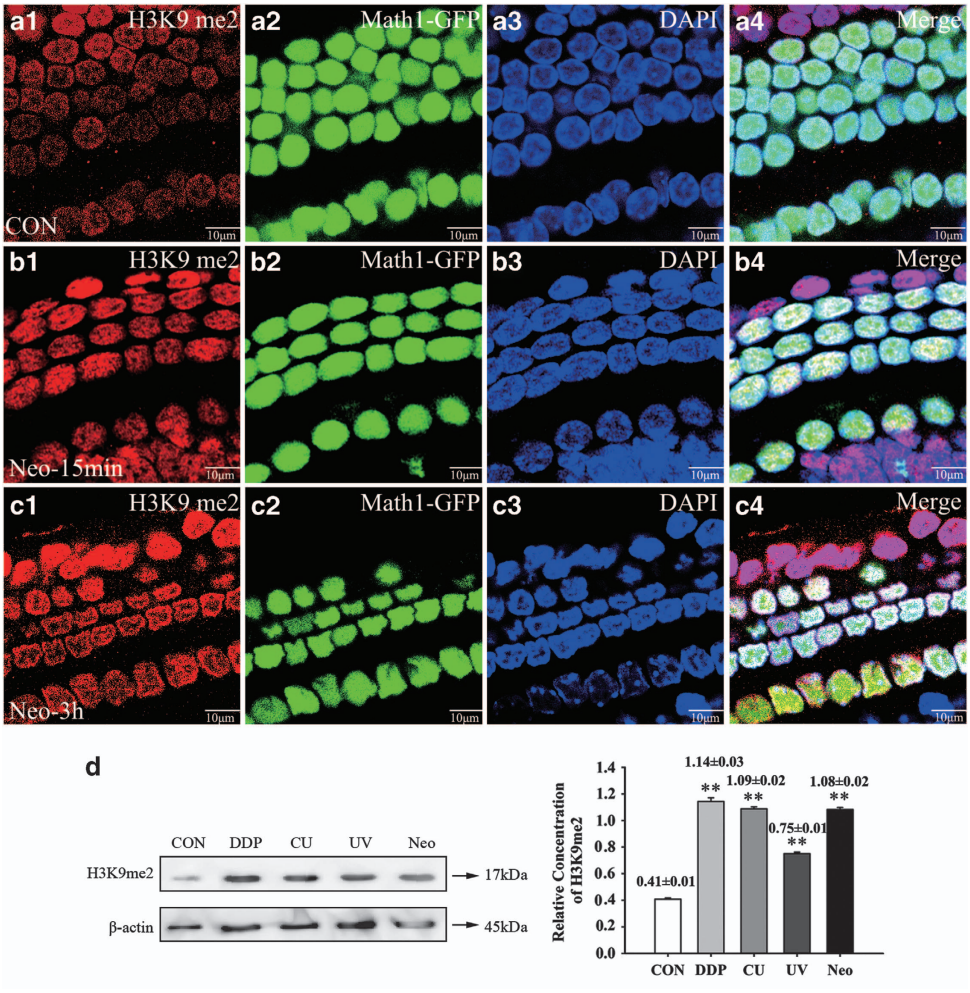

Figure 1 The global H3K9me2 levels increased rapidly upon hair cell damage. (**a**) H3K9me2 immunofluorescence was detected as punctuate staining in normal hair cells cultured as organ culture in serum-free medium. (**b** and **c**) The relative fluorescent intensity of H3K9me2 increased significantly after the addition of 1 mM neomycin for 15 min or 3 h when compared with the untreated group. (**d**) The H3K9me2 level increased after all of the following treatments: 100 μM cisplatin treatment for 3 h, 50 μM copper (CU) treatment for 3 h, ultraviolet (UV) irradiation for 15 min, or 1 mM neomycin treatment for 3 h, as confirmed by western blot analysis ($n = 12$ per group in each trial) and quantified by the grey-degree numerical value in the form of mean ± S.E. values obtained from three replicates. Shown in the images is the middle turn segment. The red spots represent the H3K9me2 signal, the green fluorescence shows staining of the hair cells and the nuclei are labelled with 4,6-diamidino-2-phenylindole (DAPI). Bar = 10 μm. $^{**}P < 0.01$. DDP; cisplatin; CON, control group

We next examined the H3K9me2 modification in three other hair cell injury models: cochlear epithelial cells were treated with 100 μM cisplatin for 3 h, with 50 μM copper for 3 h, or with ultraviolet rays for 15 min, using the 3-h treatment of 1 mM neomycin as a positive control. Western blot analysis confirmed the increase of H3K9me2 in the organ of Corti following all four types of damage (Figure 1d).

Pharmacological inhibition of G9a/GLP by BIX01294 leads to decreased H3K9me2 in cochlear epithelium. BIX01294 is a selective inhibitor of G9a/GLP, two major euchromatin histone methyltransferases responsible for H3K9me2. We examined the H3K9me2 level following BIX01294 treatment using immunofluorescence staining. The H3K9me2 level in hair cells decreased significantly after 24 h of incubation with 2 μM BIX01294 when compared with the untreated group (Figures 2a–c). Moreover, a dose-dependent effect was observed with varying BIX01294 concentrations (0, 2, and 10 μM) as determined by semi-quantitative western blot analysis, using total histone H3 as the loading control (Figure 2d). Obvious loss of hair cells was not observed in the low-concentration (2 μM) BIX01294 treatment group, but hair cell loss was found at the high concentration (10 μM) to a mild extent (Figure 2c). Therefore, we chose a concentration of 2 μM BIX01294 for further analysis.

Inhibition of G9a/GLP renders hair cells resistant to loss induced by neomycin. As the H3K9me2 modification increased rapidly upon neomycin-induced hair cell damage preceding cell death, we hypothesised that such epigenetic modulation may contribute to the onset of active apoptosis of the hair cells. We thus investigated whether suppression of H3K9me2 by BIX01294 could protect hair cells from aminoglycoside -induced hair cell loss. Four groups of experiments were conducted with the organ of Corti: 24 h 2 μM BIX01294 pre-treatment before neomycin treatment for 4 h; co-treatment of 2 μM BIX01294 and neomycin for 4 h;

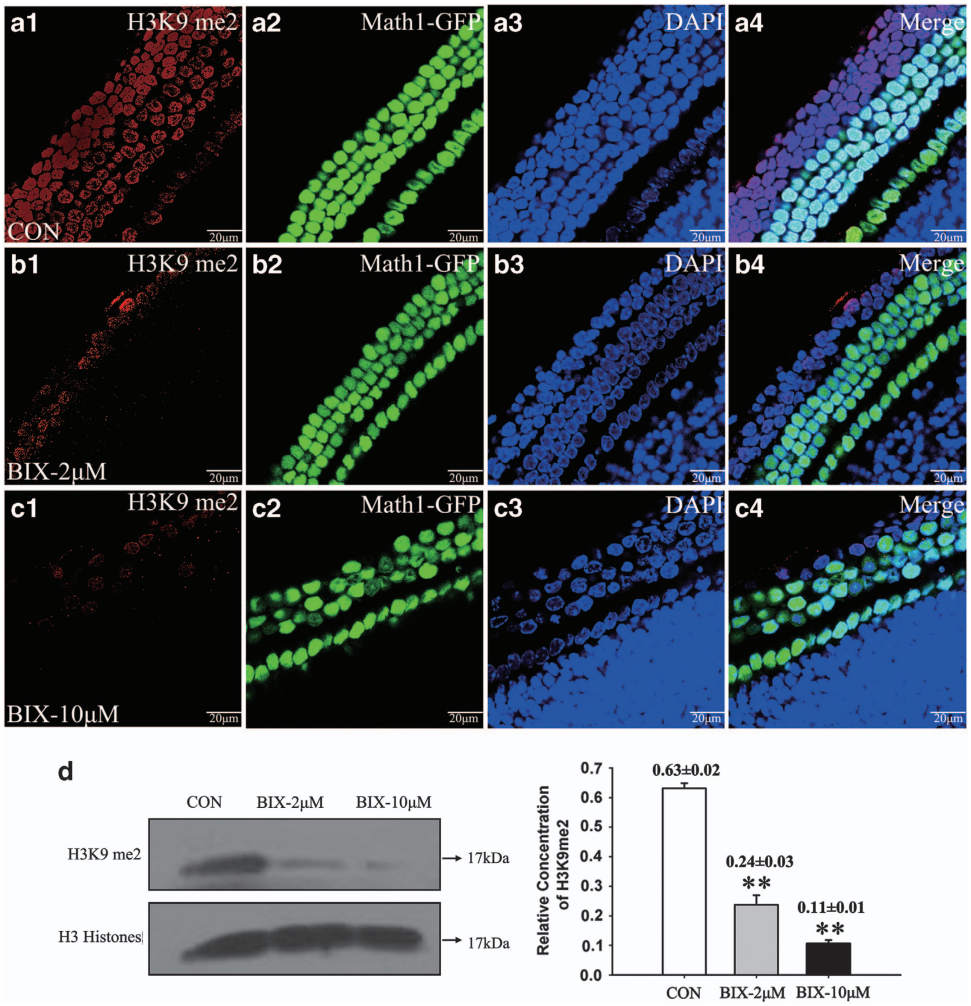

Figure 2 The H3K9me2 level decreased with BIX01294 treatment in hair cells. (**a**) H3K9me2 level is relatively uniform across the hair cell epithelium within the organs of Corti cultured in serum-free medium. Bar = 20 μm. (**b**) H3K9me2 significantly decreased with the addition of 2 μM BIX01294 for 24 h. Bar = 20 μm. (**c**) Hair cell loss was observed in the presence of 10 μM BIX01294 for 24 h in the basal segment. Bar = 20 μm. (**d**) The dose-dependent inhibition of H3K9me2 in cultured organ of Corti was confirmed by western blot analysis ($n = 12$ per group) and quantified by the grey-degree numerical value from three replicates. Analysis of variance and SNK-q test, $^{**}P < 0.01$. DAPI, 4,6-diamidino-2-phenylindole. CON, control group

24 h 2 μM BIX01294 post-treatment after neomycin for 4 h; and the neomycin-only treatment for 4 h as the control group. The mean survival rates of the hair cells across various segments of the organ of Corti are detailed in Supplementary Table S1. Significantly, more surviving hair cells and less apoptotic bodies were found in the pre-treatment group than the other three groups in the middle and basal segments (ANOVA and SNK-q test, *P*-value <0.01; Figures 3a–l). The number of surviving hair cells in the pre-treatment group was also significantly higher than in the neomycin-only controls (ANOVA and SNK-q test, *P*-value <0.01; Figure 3m), whereas that in the post-treatment group it was significantly lower than neomycin-only controls (ANOVA and SNK-q test, *P*-value <0.01). Apparent hair cell loss was not found in the apical segment of the organ of Corti in any of the four groups.

To exclude the possibility of BIX01294 off-target effect, we treated the cultured organs of Corti with another selective and potent G9a/GLP inhibitor UNC0638.[15] Similar otoprotection was observed in the UNC0638 pre-treatment group (Figure 4), confirming that the otoprotection of BIX01294 and UNC0638 likely executes through G9a/GLP inhibition before aminoglycoside treatment.

To further investigate whether the otoprotective effect of BIX01294 can be extended to other hair cell-loss models, we examined it in cisplatin-induced hair cell-injury model. Explant culture of organ of Corti were pre-treated with 2 μ BIX01294 then challenged with cisplatin for 4 h or directly challenged with cisplatin for 4 h as the control. The mean number of surviving hair cells and apoptotic bodies across various segments of the organ of Corti are counted and shown in Figure 5. We observed significant otoprotection effect of BIX01294 (ANOVA and SNK-q test, *P*-value <0.01) in cisplatin-induced hair cell-loss model.

BIX01294 does not interfere with the uptake of aminoglycosides or hair cell function. We next investigated whether BIX01294 interferes with aminoglycoside uptake by monitoring the uptake of gentamicin tagged with Texas Red (GTTR) or the uptake of a membrane permeable probe FM1-43FX. GTTR efficiently entered hair cells in the cultured organs of Corti after 30 min of incubation at 37 °C both in the control group (Figure 6a) and in the BIX01294 pre-treatment group (Figure 6b). Hair cells treated with or without BIX01294 were both able to effectively uptake FM1-43FX (Figures 6c and d). These data indicated that BIX02194 does not interfere with aminoglycoside uptake in hair cells.

BIX01294 treatment prevents the apoptotic process induced by aminoglycosides. To assess whether the resistance to neomycin injury by BIX01294 pre-treatment is achieved through the inhibition of apoptosis induced by aminoglycosides, we investigated the mitochondrial function by examining the distribution of tetramethylrhodamine methyl ester (TMRM), a fluorescent lipophilic cation, in cochlear epithelium with or without BIX01294 pre-treatment. We found

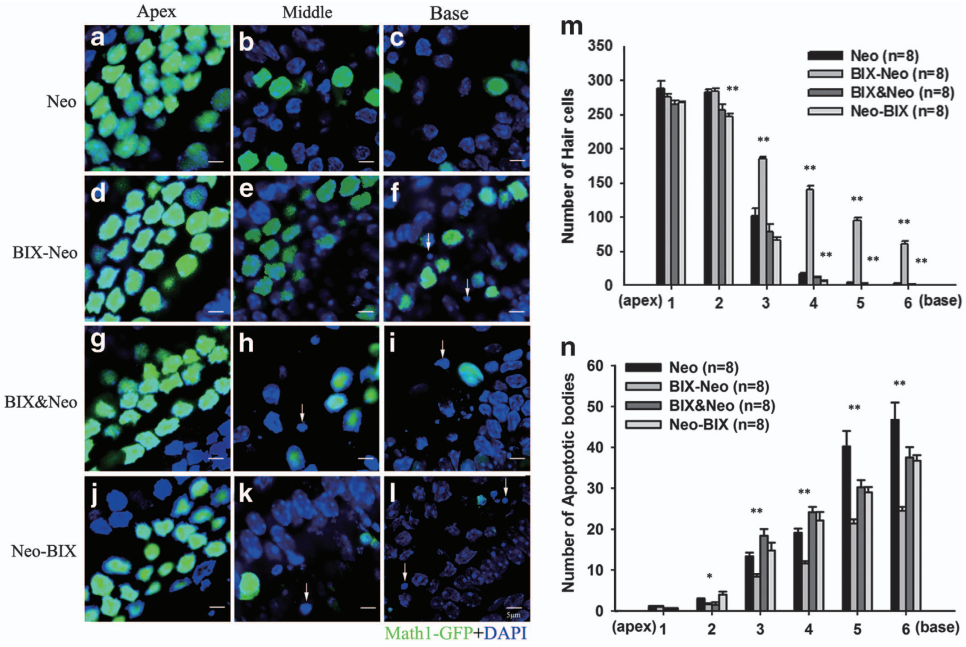

Figure 3 Assessment of hair cell survival and apoptosis upon neomycin treatment with or without BIX01294. (**a–l**) Organs of Corti were cultured in serum-free medium. They were either treated with neomycin alone (Neo), neomycin with BIX01294 pre-treatment (BIX-Neo), neomycin and BIX01294 co-treatment (co-treatment), or neomycin with BIX01294 post treatment (Neo-BIX). Shown here are the confocal images of the apical, middle, and basal turns from these four groups, respectively. The hair cells were labelled with Math1-GFP (Math1-green fluorescent protein; green), and the nuclei were DAPI (4,6-diamidino-2-phenylindole) stained (blue). Arrows in **f**, **h**, **i**, **k**, and **l** indicate the apoptotic bodies with condensed or fragmented nuclei. Bar = 5 μm. (**m**) Quantitative analysis of hair cell protection by BIX01294. The samples were divided into six segments of equal length, which was called segment 1, 2, 3, 4, 5, and 6 from apex to base. We counted the number of hair cells in each visual field with the same length of each segment for each treatment group, data are expressed as mean ± S.E. (the length is 360 μm, $n=8$ per group, $^*P<0.05$, $^{**}P<0.01$.). (**n**) Quantification of the apoptotic bodies (the length is 360 μm, $n=8$ per group, $^*P<0.05$, $^{**}P<0.01$)

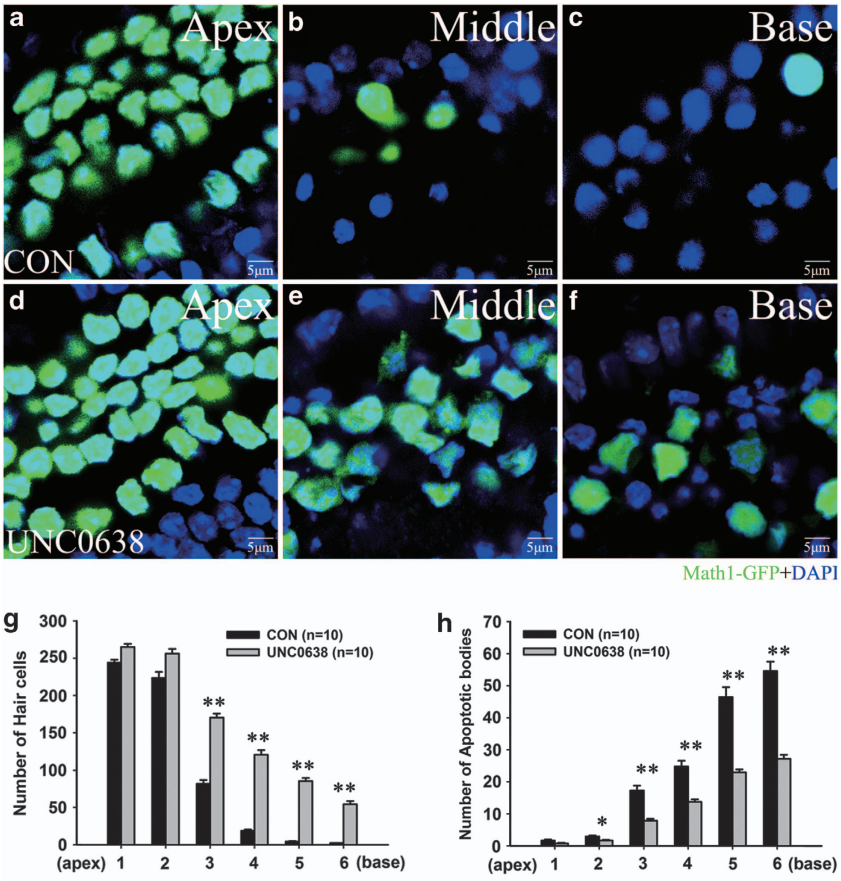

Figure 4 Quantification of hair cells and apoptotic bodies induced by neomycin with or without UNC0638 pre-conditioning. (**a**–**f**) Confocal images of the apical, middle, and basal turns in the control group and UNC0638 pre-conditioned group. The hair cells were labelled with Math1-GFP (Math1-green fluorescent protein), and the nuclei were DAPI (4,6-diamidino-2-phenylindole) stained (blue). Bar = 5 μm. (**g** and **h**) Quantification of the hair cells and apoptotic bodies was performed the same as above (the length is 360 μm, $n = 10$ per group, $^{*}P < 0.05$, $^{**}P < 0.01$). CON, control group

that the organs of Corti pre-conditioned with BIX01294 showed higher levels of visible TMRM fluorescence than the neomycin-only treated tissues (Figures 7a–c).

We next examined the expression of cleaved caspase-3, which is a late effector of apoptosis and a major mediator of aminoglycoside-induced apoptosis in auditory hair cells.[19] We found that BIX01294 pre-treated samples showed much lower expression of cleaved caspase-3 than the neomycin-only control group in both immunofluorescence and western blot analyses (Figures 7d–f). Together with the TMRM results, this indicated that pre-treatment of BIX01294 may suppress the apoptotic cascade induced by the aminoglycosides.

BIX01294 protects hair cells from aminoglycoside-induced cell damage *in vivo*. To test whether BIX01294 could prevent hair cell loss induced by aminoglycoside *in vivo*, we performed a self-controlled *in vivo* experiment in a mouse model of hair cell damage (Supplementary Figure S1). Scanning electron microscope (SEM) was used to examine the surface morphology of the organs of Corti following the physiological analysis of the hearing thresholds by ABR to assess hair cell functions. In the neomycin-only treated cochleae, the stereocilia fusions were primarily observed in the apical segment, while the stereocilia bundle loss was apparent in the middle and basal segments, accompanying a massive loss of outer hair cells (Figures 8a–f). The contralateral cochleae pre-treated with BIX01294 were slightly less damaged, with more surviving stereocilia bundles in the basal segment (Figures 8g–l). The number of surviving hair cells, as quantified by Myosin-7-positive cells, was significantly higher in the BIX01294 pre-treated ears than in the neomycin-only ears (P-value = 0.011, P-value < 0.001, and P-value < 0.001 in the apical, middle, and basal sections, respectively) (Figure 8m). In addition, the 'transitional' zone in the BIX01294 pre-treated ears was much closer to the basal border within the middle segment (Figure 8n). Within this region, we observed some remaining apoptotic nuclei with marginated and condensed chromatin, as shown by Hoechst 33342 staining (Figures 8h, i, and l). Concordant with previous findings, the neomycin treatment caused a significant ABR-threshold shift, whereas BIX01294 pre-conditioning ameliorated this threshold shift (Supplementary Figure S2). Quantitative analysis of the ABR showed that the amelioration was at least 15 dB at both 8000 and 16 000 Hz (P-value = 0.0011 and P-value < 0.001, respectively) (Figure 8o).

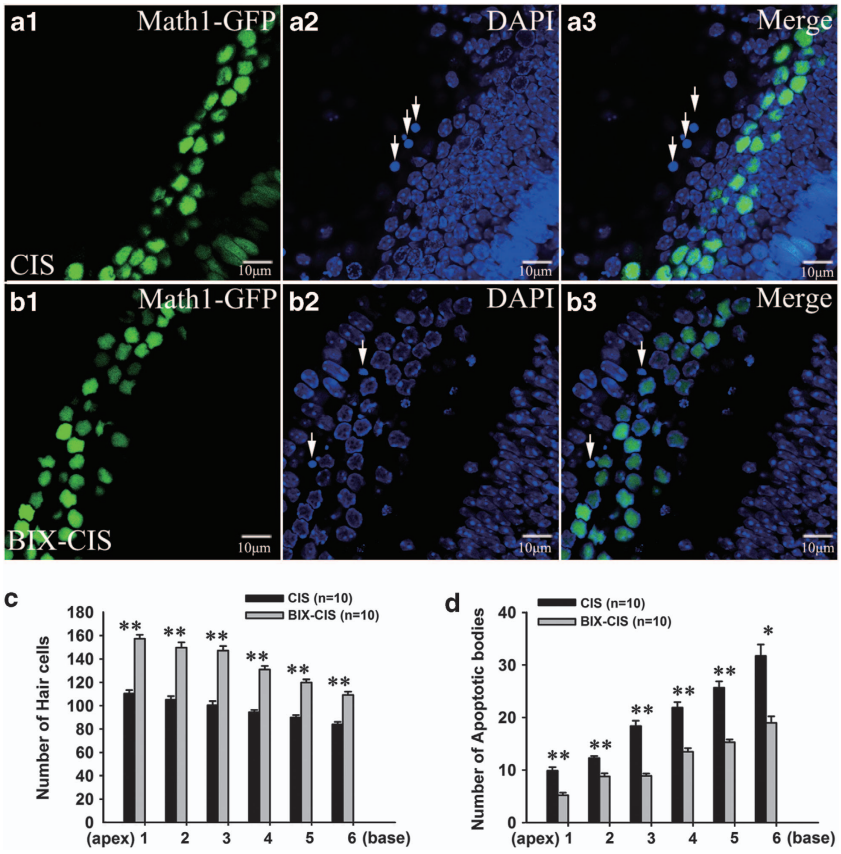

Figure 5 Quantification of hair cells and apoptotic bodies induced by cisplatin with or without BIX01294 pre-conditioning. (**a** and **b**) Confocal images of the middle turns in the control group and BIX01294 pre-conditioned group. The hair cells were labelled with Math1-GFP (Math1-green fluorescent protein) and the nuclei were DAPI (4,6-diamidino-2-phenylindole) stained (blue). Arrows in **a** and **b** indicate the apoptotic bodies with condensed or fragmented nuclei. Bar = 5 μm. (**c** and **d**) Quantification of the hair cells and apoptotic bodies was performed the same as described in Figure 4 (the length is 360 μm, $n = 10$ per group, $^{*}P<0.05$, $^{**}P<0.01$)

Discussion

Histone modifications in various forms constitute a major force in the epigenetic regulation of gene expression. Coordinated activities of histone modification enzymes have been proposed to create a 'histone code' that controls transcription and other genome functions, such as replication and DNA repair.[20–22] In particular, histone methylation and demethylation are associated with transcription regulation, genome integrity, and epigenetic inheritance.[23] As one of the most abundant and dynamic histone modifications, H3K9me2 patterns vary greatly during development and in disease pathogenesis.[24] It has been shown that H3K9me2 levels increase during ES-cell differentiation while decreasing before the reprogramming of somatic cells to iPS,[25–27] indicating its role in cell differentiation or cell fate determination. Moreover, the enrichment of H3K9me2 is associated with various types of perpetuating malignancy in cancer cells,[28,29] as well as in hypoxic stress, which may function through various pathways.[30,31]

In the present study, we first examined the H3K9me2 level upon aminoglycoside-induced hair cell damage in cultured cochlear explants. We found that neomycin treatment induced a rapid increase of the H3K9me2 level in the organ of Corti before detectable apoptosis. The enrichment of H3K9me2 disappeared after 24 h of prolonged neomycin treatment, largely due to severe loss of hair cells. Thus we hypothesised that the increased H3K9me2 level may contribute to the onset of active cell death in hair cell injury. Previous studies also found the enrichment of H3K9me2 or G9a in different cancer cells following hypoxia, although the chronological order of the apoptosis and the H3K9me2 upregulation has not been established.[32,33]

We then asked whether blocking this increase of H3K9me2 level can suppress the onset of the apoptotic programme induced by aminoglycoside and prevent the consequent hair cell death. Indeed, we found that inhibition of G9a/GLP by pharmacological inhibitors BIX01294 or UNC0638 blocks the rapid increase of H3K9me2 and prevents hair cell loss induced by neomycin. Peltonen *et al*.[34] confirmed that certain cancer cells are susceptible to apoptosis, which may be associated with the regulation of p53. Substantial evidence suggests that the interference of H3K9me2, which is involved in the regulation of gene expression, may influence the susceptibility or tolerance of the cells to stress. Therefore, it is possible that G9a/GLP inhibition may lead to the suppression of specific gene expression changes resulted from the histone

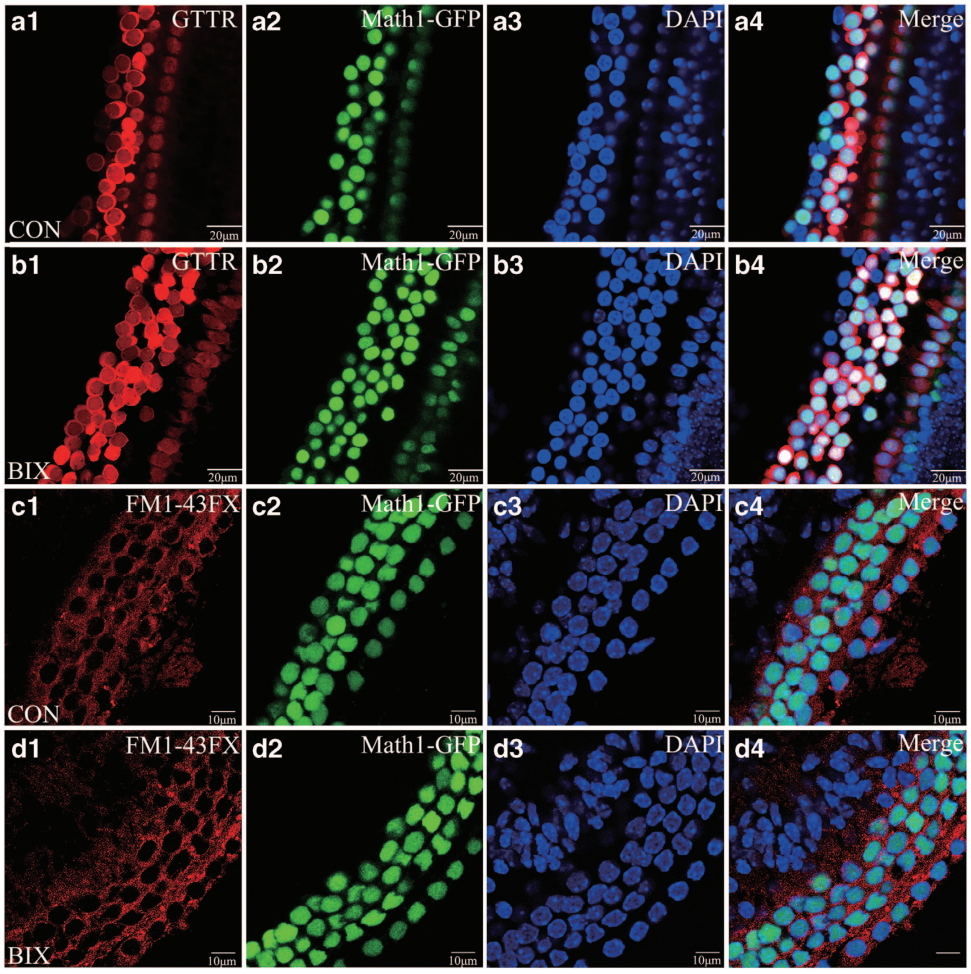

Figure 6 BIX01294 does not interfere with the uptake of the gentamicin and FM1-43FX. (**a** and **b**) Explants were incubated with GTTR for 30 min in the absence or presence of BIX01294. The red fluorescence represents GTTR, the green fluorescence represents the hair cells, and blue represents DAPI (4,6-diamidino-2-phenylindole) staining of the nuclei. Shown here are the confocal images of the middle segments of each group. Bar = 20 μm. (**c** and **d**) The hair cell function was not affected when measuring the uptake of FM1-43FX in the presence or absence of 2 μM BIX01294. GFP, green fluorescent protein

methylation imbalance caused by oto-damage induced by aminoglycosides.

We have shown that G9a/GLP inhibition by BIX01294 or UNC0638 are effective in terms of preventing hair cell damage induced by aminoglycosides both *ex vivo* and *in vivo*. However, the mechanisms of otoprotection by BIX01294 or UNC0638 remain undetermined. It was believed that apoptotic cell death, instead of necrosis, is the primary cause of hair cell death induced by aminoglycosides.[35,36] Measuring TUNEL-positive nuclei and the activated caspase-3 labelling, Taylor *et al*.[37] demonstrated that most hair cells die via a classical apoptotic pathway, and we have shown here that the caspase-dependent pathway was suppressed by BIX01294 pre-treatment. Besides caspase-3, the collapse of membrane potential of the mitochondria is another signal of early apoptosis event.[38] Our TMRM staining indicated that BIX01294 is able to prevent the neomycin-induced disruption of the mitochondrial membrane potential and may lead to new insights into the mechanism of otoprotection. The detailed effect of G9a/GLP inhibition and consequent H3K9me2 reduction on mitochondrial function remains unknown.

In summary, our findings revealed a novel epigenetic mechanism underlying hair cell injury. Inhibition of H3K9me2 may disrupt the apoptotic cell death programme induced by aminoglycosides and thus prevents hair cell loss. Such findings provide novel scientific insights into hair cell damage and may contribute to the development of hair cell-protection therapies. A more complete picture of signalling pathways and molecular mechanisms underlying this otoprotection should be elucidated in future studies.

Materials and Methods

In vitro studies

Animal care: Animal care and use were in accordance with the 'Guiding Directive for Humane treatment of Laboratory Animals'. The procedure was approved by the Chinese Science Academy Committee on Care and Use of Animals and performed using accepted veterinary standards. Post-natal day-2 transgenic mice containing the *Math1-GFP* transgene were used in the *in vitro* experiments. The mouse line was a generous gift from M. Charles Liberman, as previously described.[39]

Tissue culture and compound administration: Dissection and culture of the mouse cochlear explant were performed as previously described.[40] The tissues were

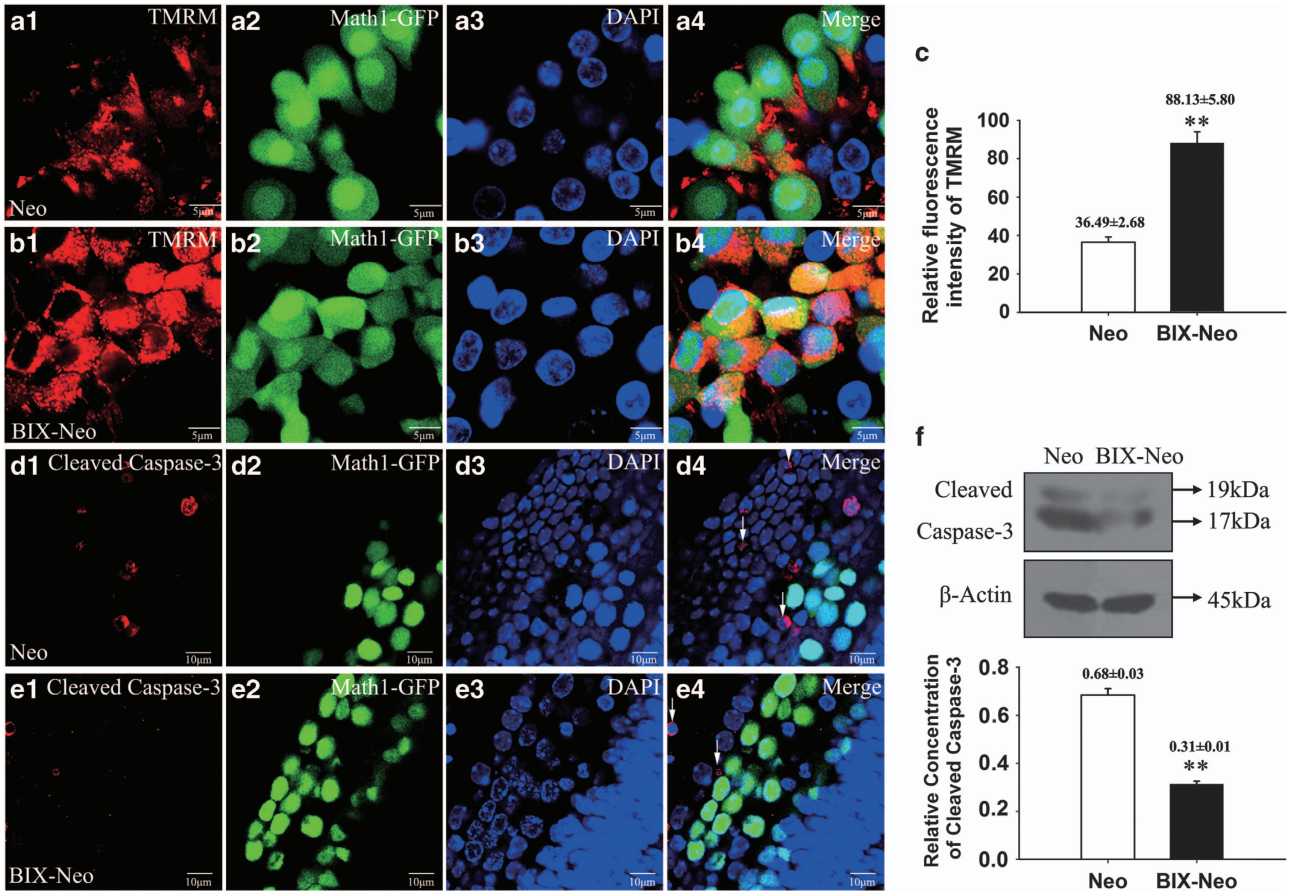

Figure 7 BIX01294 treatment affects mitochondrial apoptosis pathway. (**a** and **b**) Mitochondrial membrane permeability (MMP) staining of the organs of Corti in neomycin-induced hair cell damage model with or without BIX01294. The red fluorescence shows the live-cell imaging of the MMP tagged with TMRM, the green fluorescence represents the hair cells labelled with Math1-GFP (Math1-green fluorescent protein), and blue represents DAPI (4,6-diamidino-2-phenylindole) staining of the nuclei. Shown here are the confocal images of the middle segments of each group. The TMRM staining in the hair cells decreased significantly with the neomycin-only treatment, whereas it only slightly decreased in the presence of BIX01294. Bar = 20 μm. (**c**) The relative fluorescence intensity of TMRM in the control group and BIX01294 pre-conditioned group ($n = 3$ per group). (**d** and **e**) The level of cleaved caspase-3 decreased in the presence of 2 μM BIX01294 when compared with the neomycin-only-treated organ of Corti. Shown here are the confocal images of the middle segments of each group. Bar = 20 μm. (**f**) The average level of cleaved caspase-3 was measured using western blot ($n = 12$ per group in each trial) and plotted in the form of mean ± S.E. values obtained from three replicates. β-actin was used as the loading control

cultured on poly-L-lysine-treated (Sigma-Aldrich, St. Louis, MO, USA) cover slides filled with 30 μl of serum-free medium, which consists of DMEM/F12 basal medium supplemented with N2 and B27 solutions (Invitrogen, Carlsbad, CA, USA). The cover slides were placed in a 35-mm dish. To obtain a flat basilar membrane surface, the Reissner's membrane, spiral ligament, and stria vascular were carefully removed. After the tissues were attached to the slides, 1.5 ml of medium was added to the petri dish. Half of the medium was replenished every other day.

After the tissues were attached to the slides, they were incubated with the medium containing specific G9a/GLP inhibitors, 2 μM BIX01294 or 2 μM UNC0638 (Sigma-Aldrich), neomycin (1 mM) or a combination of both for designated times, as shown in Supplementary Tables S2 and S3.

Quantification of the surviving hair cells: To quantify the viable hair cells, the entire cochlea was divided into six segments of equal length, which were called segment 1, 2, 3, 4, 5, and 6 from apex to the base. The hair cells marked with Math1-GFP in the central field of view (360 μm in each segment) were counted. Data are presented as means ± S.E.M. ANOVA, the SNK-q test, or Student's *t*-test were performed to analyse the compound effects. Differences between groups were considered statistically significant when $P < 0.05$.

Apoptotic labelling: Apoptotic cells were detected by the presence of nuclear condensation or fragmentation by using DAPI staining (Sigma-Aldrich), which was performed as previously described.[41] This was also confirmed by TUNEL labelling (Fluorescein In situ Cell death detection kit, Millipore, Bedford, MA, USA) according to the manufacturer's instruction. Quantification of the apoptotic cells in the cochlea was performed in the same way as described above.

GTTR and FM1-43FX uptake: FM1-43 can enter hair cells as previously described.[42,43] To measure aminoglycoside uptake, the cochlear organs (neo group and pre-treatment group) were cultured for 24 h as described above. After rinsing with PBS, they were incubated with the same serum-free medium containing GTTR (10 mM) for 30 min or FM1-43FX (Molecular Probes, Eugene, OR, USA) for 3 min. After incubation, the cochlea was fixed for analysis using fluorescent microscopy.

Live-cell Imaging of mitochondrial membrane permeability: The cochlear organs (neo group and pre-treatment group) were cultured and incubated in serum-free medium containing neomycin (1 mM) for 30 min, followed by serum-free medium containing TMRM (25 nM) for 30 min. The tissues were then washed with PBS before imaging analysis.

Immunohistochemistry: Samples were fixed in 4% paraformaldehyde in PBS for 2 h at room temperature, followed by rinsing three times in PBS. The tissues were then permeabilized in 0.2% Triton X-100 in PBS for 30 min at room temperature, blocked with 10% donkey serum in PBS for 1 h at 37 °C, and then incubated with the primary antibody (diluted in blocking solution) at 4 °C for 48 h. After washing

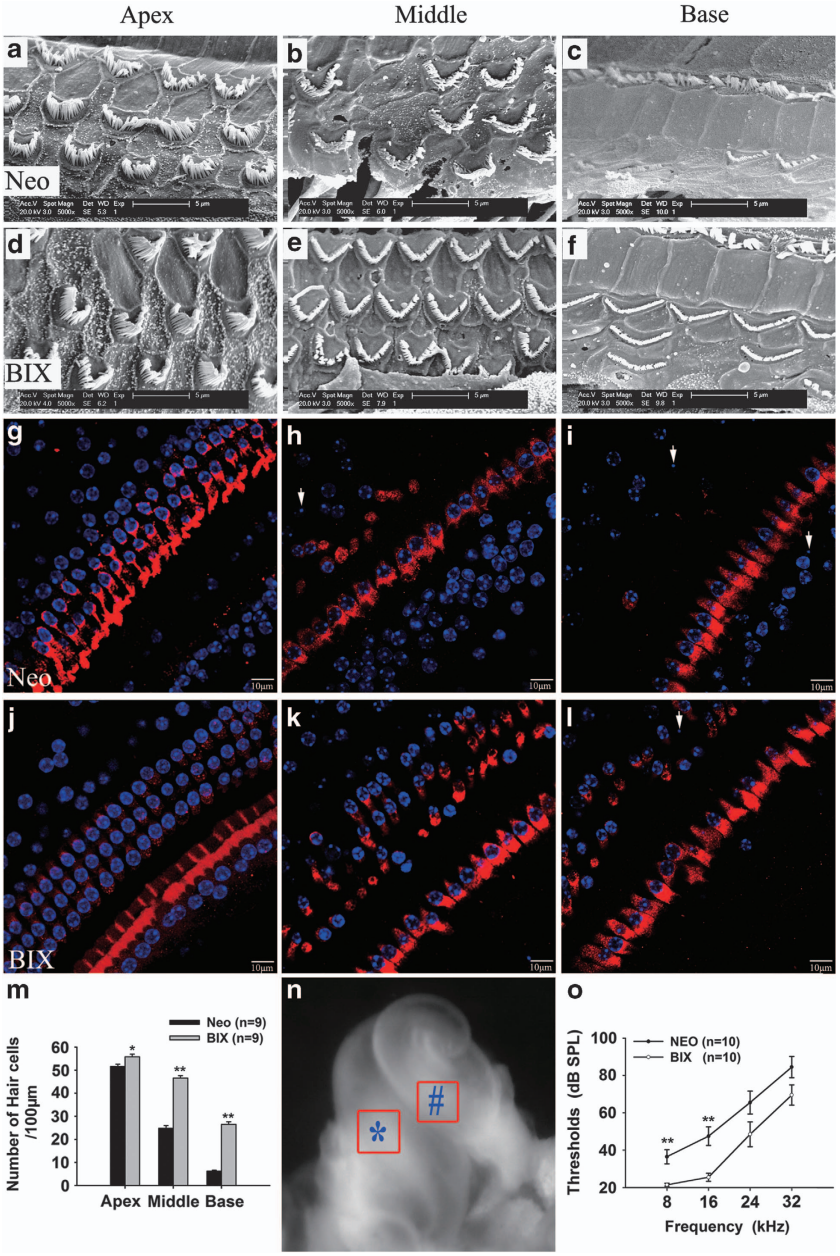

Figure 8 Inhibition of G9a/GLP protects auditory hair cell death in the organ of Corti *in vivo*. (**a–f**) SEM examination of the stereocilia in the organ of Corti was performed from the apical turn to the basal turn in the neomycin-exposed animal with or without the BIX01294 pre-treatment. There is less severe hair cells loss in the BIX01294 pre-treatment group as compared with the untreated group. Bar = 5 μm. (**g–l**) Similar results were obtained using confocal microscopy of Myosin7a (red) and nuclear (blue) staining. Bar = 10 μm. (**m**) Quantification of the surviving hair cells at the apical, middle, and basal turns of the cochlea of each group. The length used for the statistical analysis was 100 μm, $n = 9$ in each group. Data are expressed as mean ± S.E. (Student's *t*-test, $^{*}P < 0.05$, $^{**}P < 0.01$). (**n**) A sketch was drawn to show the 'transitional' zone for the different conditions: BIX-Neo (#) *versus* Neo (*). (**o**) The mean ABR threshold was compared between left and right ears, that is, the ears with or without BIX01294 pre-treatment, $n = 10$ in each group. Data are expressed as mean ± S.E. (Student's *t*-test, $^{*}P < 0.05$, $^{**}P < 0.01$)

away the primary antibody, the cultures were incubated with fluorescent dye-conjugated secondary antibody for 1 h at 37 °C to visualise the signal. The primary antibodies used were cleaved caspase-3 antibody (Cell Signaling Technology, Beverly, MA, USA, rabbit polyclonal, dilution 1 : 200) and anti-H3K9me2 antibody (Abcam, Cambridge, MA, USA, mouse monoclonal, dilution 1 : 200). The secondary antibodies were Alexa Fluor 555 donkey anti-mouse or rabbit IgG (Invitrogen, Carlsbad, CA, USA, dilution 1 : 400). The nuclei were labelled by DAPI staining. The images were captured using a Leica confocal microscope (Heidelberg, Germany).

Western blot analysis. For western blot analysis, total protein was isolated from each of the 12 specimens using the AllPrep DNA/RNA/Protein Mini Kit (QIAGEN, Hilden, Germany) according to the manufacturer's instructions. The protein concentrations were determined using a BCA protein kit (Beyotime, Jiangsu, China). In all, 50 μg of the samples from each group were separated by 12% SDS-PAGE. After electrophorsis, the proteins were transferred to PVDF membranes (Millipore). The membranes were blocked with 5% non-fat dried milk in TBST for 1 h at room temperature. After washing, the primary antibodies, including cleaved caspaspe-3 antibody (dilution 1 : 1000), anti-H3K9me2 antibody (dilution 1 : 1000),

β-actin antibody (Cell Signaling Technology, Beverly, MA, USA, rabbit polyclonal, dilution 1 : 1000), and anti-histone H3 antibody (Cell Signaling Technology, rabbit polyclonal, dilution 1 : 1000), were added into the blocking buffer overnight at 4 °C. After three times rinsing (10 min each) with TBST, the membranes were incubated with the blocking buffer containing the HRP-conjugated secondary antibody at a concentration of 1 : 5000 (Supersignal West, Pierce, Rockford, IL, USA) for 1 h at room temperature. The immunoreactive bands were visualised using an ECL kit (Pierce). To quantify the relative levels of the protein, images of specific protein bands were assessed by the grey-degree numerical value.

In vivo studies

Experimental protocol: Wild-type C57BL/6 mice were used for the *in vivo* studies. All animal studies were in accordance with the 'Guiding Directive for Humane treatment of Laboratory Animals. As shown in Supplementary Table S4, we applied a retro-auricular surgical approach in 5-day-old mice following anaesthesia. To evaluate the otoprotection of G9a/GLP inhibition, the left ears were pre-treated with BIX01294 while the right ears were left untreated as the self-control. A piece of gelfoam (1 mm^3) soaked with BIX01294 (10 mM, 2 μl) was positioned onto the round window niche through the small hole in the bulla, resulting in an approximate applied dose of 25 μg of the drug in each pre-treated ear. The inferior skin incision was then closed with four silk sutures. Two days after administration of BIX01294, neomycin was injected subcutaneously once a day for 4 consecutive days. The neomycin was dissolved in saline at a concentration of 20 mg/ml so that a final dose of 200 mg of neomycin/kg of body weight was obtained by injecting 0.01 ml/g of body weight. Dosing of the neomycin was adjusted according to the accurate weight of the animals each day. Two weeks after exposure to neomycin, the hearing threshold was evaluated by ABR measurement.

ABR: The ABR analysis was performed in anaesthetised (100 mg/kg ketamine and 25 mg/kg xylazine sodium, i.p.) mice to measure the hearing threshold 2 weeks after the administration of neomycin. The hearing threshold was assessed at four frequencies (8, 16, 24, and 32 kHz) in a TDT system 3 (Tucker Davies Technologies, Gainesville, FL, USA). The traditional three electrodes (stimulus, reference, and grounding electrodes) were inserted subcutaneously at the vertex cranial, homolateral mastoid process, and nasal root, respectively. To prevent the influence from the other ear, the source microphone was positioned directly inside the external auditory canal during the sound acquisition. The threshold response was defined as the lowest response that could demonstrate a reproducible waveform. If there was ambiguity about the results, the ABR would be repeated the following day. The parameters of the evoked responses and acquired signal were as follows: duration of toneburst, 5 ms; rise–fall time, 0.5 ms; stimulus frequency, 21.37/s; stacking fold (superposition times), 500–1000; magnification, 20; bandpass, 0.3–3 kHz; sound intensity variation, 5 dB; amplitude of sound pressure level (SPL), 20–95 dB.

Scanning electron microscopy: The cochlea was perfused immediately with 4% paraformaldehyde after the mouse was anaesthetised. The tissues were then immersed in 2.5% glutaraldehyde for SEM. The SEM samples were post-fixed in 1% phosphate-buffered OsO4, dehydrated in a graded ethanol series, dried and mounted on to an aluminium sheet, and sprayed with gold–palladium. SEM was performed using a Philips XL-30 (Eindhoven, the Netherlands) SEM apparatus.

Immunohistochemistry: Immunohistochemistry was performed similarly as described above. Hair cells were marked with polyclonal anti-myosin 7a (Proteus Biosciences, Ramona, CA, USA). The apoptotic bodies were detected by Hoechst 33342 (Sigma-Aldrich) to identify the condensed or fragmented nuclei.

Statistics: The results were presented as means ± S.E.M. Student's *t*-test was performed to determine statistical significance. The results were considered significant when $P < 0.05$ between the groups.

Conflict of Interest

The authors declare no conflict of interest.

Acknowledgements. We thank Chuijin Lai and Wen Li for technical assistance and Yalin Huang for the confocal technical help. We would also like to thank Dr. Haiyan Xu for critical reading and editing of the manuscript. This work was supported by grants from the Major State Basic Research Development Programme of China (973 Program) (2011CB504506, 2010CB945503), the Programme for Changjiang Scholars and Innovative Research Team in University (IRT1010), the National Natural Science Foundation of China (No. 81070793, 30901668), the Innovation Programme of Major Basic Research Project, Science and Technology Commission of Shanghai Municipality (09DJ1400602), the Programme for Outstanding Shanghai Academic Leaders (11XD1401300), and the Programme for Leading Medical Personnel in Shanghai. This study was partly supported by the Novartis-Fudan collaboration.

1. Willems PJ. Genetic causes of hearing loss. *N Engl J Med* 2000; **342**: 1101–1109.
2. Edge AS, Chen ZY. Hair cell regeneration. *Curr Opin Neurobiol* 2008; **18**: 377–382.
3. Chen P, Johnson JE, Zoghbi HY, Segil N. The role of Math1 in inner ear development: uncoupling the establishment of the sensory primordium from hair cell fate determination. *Development* 2002; **129**: 2495–2505.
4. Matsui JI, Haque A, Huss D, Messana EP, Alosi JA, Roberson DW *et al.* Caspase inhibitors promote vestibular hair cell survival and function after aminoglycoside treatment *in vivo*. *J Neurosci* 2003; **23**: 6111–6122.
5. Fraga MF, Ballestar E, Paz MF, Ropero S, Setien F, Ballestar ML *et al.* Epigenetic differences arise during the lifetime of monozygotic twins. *Proc Natl Acad Sci USA* 2005; **102**: 10604–10609.
6. Lewis MA, Quint E, Glazier AM, Fuchs H, De Angelis MH, Langford C *et al.* An ENU-induced mutation of miR-96 associated with progressive hearing loss in mice. *Nat Genet* 2009; **41**: 614–618.
7. Papp B, Plath K. Reprogramming to pluripotency: stepwise resetting of the epigenetic landscape. *Cell Res* 2011; **21**: 486–501.
8. Reik W. Stability and flexibility of epigenetic gene regulation in mammalian development. *Nature* 2007; **447**: 425–432.
9. Slotkin RK, Martienssen R. Transposable elements and the epigenetic regulation of the genome. *Nat Rev Genet* 2007; **8**: 272–285.
10. Rizzi R, Di Pasquale E, Portararo P, Papait R, Cattaneo P, Latronico MVG *et al.* Post-natal cardiomyocytes can generate iPS cells with an enhanced capacity toward cardiomyogenic re-differentation. *Cell Death Differ* 2012; **19**: 1162–1174.
11. Rice KL, Hormaeche I, Licht JD. Epigenetic regulation of normal and malignant hematopoiesis. *Oncogene* 2007; **26**: 6697–6714.
12. Zernicka-Goetz M, Morris SA, Bruce AW. Making a firm decision: multifaceted regulation of cell fate in the early mouse embryo. *Nat Rev Genet* 2009; **10**: 467–477.
13. Stark GR, Wang Y, Lu T. Lysine methylation of promoter-bound transcription factors and relevance to cancer. *Cell Res* 2011; **21**: 375–380.
14. Chang Y, Zhang X, Horton JR, Upadhyay AK, Spannhoff A, Liu J *et al.* Structural basis for G9a-like protein lysine methyltransferase inhibition by BIX-01294. *Nat Struct Mol Biol 2009; 16: 312–317.*
15. Vedadi M, Barsyte-Lovejoy D, Liu F, Rival-Gervier S, Allali-Hassani A, Labrie V *et al.* A chemical probe selectively inhibits G9a and GLP methyltransferase activity in cells. *Nat Chem Biol* 2011; **7**: 566–574.
16. Kubicek S, O'Sullivan RJ, August EM, Hickey ER, Zhang Q, Teodoro ML *et al.* Reversal of H3K9me2 by a small-molecule inhibitor for the G9a histone methyltransferase. *Mol Cell* 2007; **25**: 473–481.
17. Ma AN, Huang WL, Wu ZN, Hu JF, Li T, Zhou XJ *et al.* Induced epigenetic modifications of the promoter chromatin silence survivin and inhibit tumor growth. *Biochem Biophys Res Commun* 2010; **393**: 592–597.
18. Varier RA, Timmers HT. Histone lysine methylation and demethylation pathways in cancer. *Biochim Biophys Acta* 2011; **1815**: 75–89.
19. Eshraghi AA, Wang J, Adil E, He J, Zine A, Bublik M *et al.* Blocking c-Jun-N-terminal kinase signaling can prevent hearing loss induced by both electrode insertion trauma and neomycin ototoxicity. *Hear Res* 2007; **226**: 168–177.
20. Taverna SD, Li H, Ruthenburg AJ, Allis CD, Patel DJ. How chromatin-binding modules interpret histone modifications: lessons from professional pocket pickers. *Nat Struct Mol Biol* 2007; **14**: 1025–1040.
21. Berger SL. The complex language of chromatin regulation during transcription. *Nature* 2007; **447**: 407–412.
22. Jenuwein T, Allis CD. Translating the histone code. *Science* 2001; **293**: 1074–1080.
23. Klose RJ, Zhang Y. Regulation of histone methylation by demethylimination and demethylation. *Nat Rev Mol Cell Biol* 2007; **8**: 307–318.
24. Bhaumik SR, Smith E, Shilatifard A. Covalent modifications of histones during development and disease pathogenesis. *Nat Struct Mol Biol* 2007; **14**: 1008–1016.
25. Feldman N, Gerson A, Fang J, Li E, Zhang Y, Shinkai Y *et al.* G9a-mediated irreversible epigenetic inactivation of Oct-3/4 during early embryogenesis. *Nat Cell Biol* 2006; **8**: 188–194.
26. Lin W, Dent SY. Functions of histone-modifying enzymes in development. *Curr Opin Genet Dev* 2006; **16**: 137–142.

27. Li Y, Zhang Q, Yin X, Yang W, Du Y, Hou P *et al.* Generation of iPSCs from mouse fibroblasts with a single gene, Oct4, and small molecules. *Cell Res* 2011; **21**: 196–204.
28. Kondo Y, Shen L, Suzuki S, Kurokawa T, Masuko K, Tanaka Y *et al.* Alterations of DNA methylation and histone modifications contribute to gene silencing in hepatocellular carcinomas. *Hepatol Res* 2007; **37**: 974–983.
29. Rodriguez-Paredes M, Esteller M. Cancer epigenetics reaches mainstream oncology. *Nat Med* 2011; **17**: 330–339.
30. Chen H, Yan Y, Davidson TL, Shinkai Y, Costa M. Hypoxic stress induces dimethylated histone H3 lysine 9 through histone methyltransferase G9a in mammalian cells. *Cancer Res* 2006; **66**: 9009–9016.
31. Tausendschon M, Dehne N, Brune B. Hypoxia causes epigenetic gene regulation in macrophages by attenuating Jumonji histone demethylase activity. *Cytokine* 2011; **53**: 256–262.
32. Iaccarino I, Martins LM. Therapeutic targets in cancer cell metabolism and death. *Cell Death Differ* 2011; **18**: 565–570.
33. Tausendschön M, Dehne N, Brüne B. Hypoxia causes epigenetic gene regulation in macrophages by attenuating Jumonji histone demethylase activity. *Cytokine* 2011; **53**: 256–262.
34. Peltonen K, Kiviharju TM, Jarvinen PM, Ra R, Laiho M. Melanoma cell lines are susceptible to histone deacetylase inhibitor TSA provoked cell cycle arrest and apoptosis. *Pigment Cell Res* 2005; **18**: 196–202.
35. Cunningham LL, Cheng AG, Rubel EW. Caspase activation in hair cells of the mouse utricle exposed to neomycin. *J Neurosci* 2002; **22**: 8532–8540.
36. Selimoglu E. Aminoglycoside-induced ototoxicity. *Curr Pharm Des* 2007; **13**: 119–126.
37. Taylor R, Nevill G, Forge A. Rapid hair cell loss: a mouse model for cochlear lesions. *J Assoc Res Otolaryngol* 2008; **9**: 44–64.
38. Green DR, Reed JC. Mitochondria and apoptosis. *Science* 1998; **281**: 1309–1312.
39. Lumpkin EA, Collisson T, Parab P, Omer-Abdalla A, Haeberle H, Chen P *et al.* Math1-driven GFP expression in the developing nervous system of transgenic mice. *Gene Expr Patterns* 2003; **3**: 389–395.
40. Wang Z, Jiang H, Yan Y, Wang Y, Shen Y, Li W *et al.* Characterization of proliferating cells from newborn mouse cochleae. *Neuroreport* 2006; **17**: 767–771.
41. Hakem R, Hakem A, Duncan GS, Henderson JT, Woo M, Soengas MS *et al.* Differential requirement for caspase 9 in apoptotic pathways in vivo. *Cell* 1998; **94**: 339–352.
42. Angunsri N, Taura A, Nakagawa T, Hayashi Y, Kitajiri S, Omi E *et al.* Insulin-like growth factor 1 protects vestibular hair cells from aminoglycosides. *Neuroreport* 2011; **22**: 38–43.
43. Gale JE, Marcotti W, Kennedy HJ, Kros CJ, Richardson GP. FM1-43 dye behaves as a permeant blocker of the hair-cell mechanotransducer channel. *J Neurosci* 2001; **21**: 7013–7025.

Supplementary Information accompanies the paper on Cell Death and Disease website (http://www.nature.com/cddis)